

Resistance to Diet-Induced Obesity in Mice with Synthetic Glyoxylate Shunt

Jason T. Dean, Linh Tran, Simon Beaven, Peter Tontonoz, Karen Reue, Katrina M. Dipple, and James C. Liao

1) Supplemental Figures (Figures S1-S9)

Figure S1.....	2
Figure S2.....	3
Figure S3.....	4
Figure S4.....	5
Figure S5.....	6
Figure S6.....	7
Figure S7.....	8
Figure S8.....	9
Figure S9.....	10

2) Supplemental Tables (Tables S1-S6)

Table S1.....	11
Table S2.....	12-13
Table S3.....	14-15
Table S4.....	16
Table S5.....	17

3) Experimental Procedures

Reactions.....	18-19
Plasmid Construction.....	20-21
Cell Culture.....	21-22
Metabolite Analysis.....	22
Gluconeogenesis Assay.....	23
Fatty Acid Fluorescence Uptake Assay.....	23
¹⁴ CO ₂ Production from [U- ¹⁴ C] Palmitate.....	24
siRNA Knockdown of Malic Enzyme.....	24-25
Real-Time PCR.....	25
Microarray Expression Analysis.....	25-27
Western Blotting.....	27-28
Animal Care.....	28
Tail Vein Injections.....	28-29
Experimental Protocol-1.....	29
Experimental Protocol-2.....	30

Malonyl-CoA Assay.....	30-31
Leptin and Insulin ELISA.....	31
Liver Total ATP.....	31
Liver TG Content.....	32-33
Indirect Calorimetry, Feeding and Activity.....	32-33
References.....	34-35

Supplemental Figures

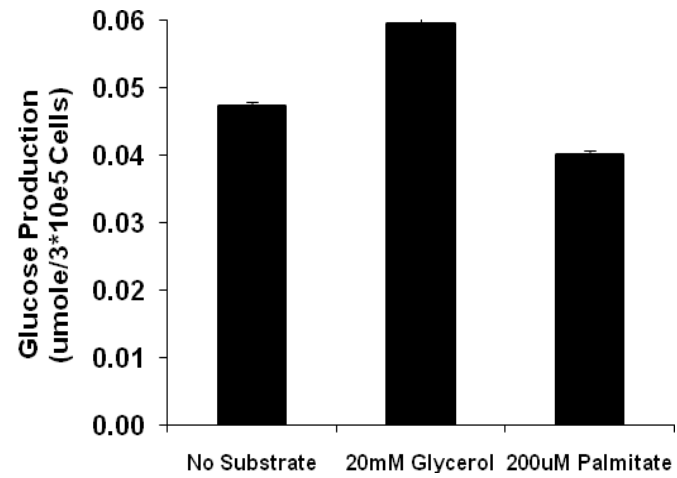


Figure S1. Glucose production in ACE cells with different gluconeogenic substrates was measured as described in Methods. Mean \pm SEM; n = 2.

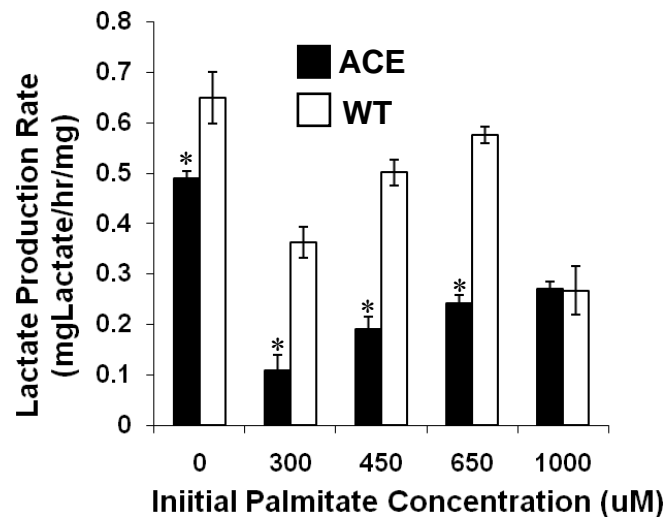


Figure S2. Lactate production was measured in ACE and WT cells over a range of palmitate concentrations. ACE cells consume less glucose than WT and produce less lactate. * $p < 0.05$ compared to corresponding WT control. Mean \pm SEM; $n = 3-6$.

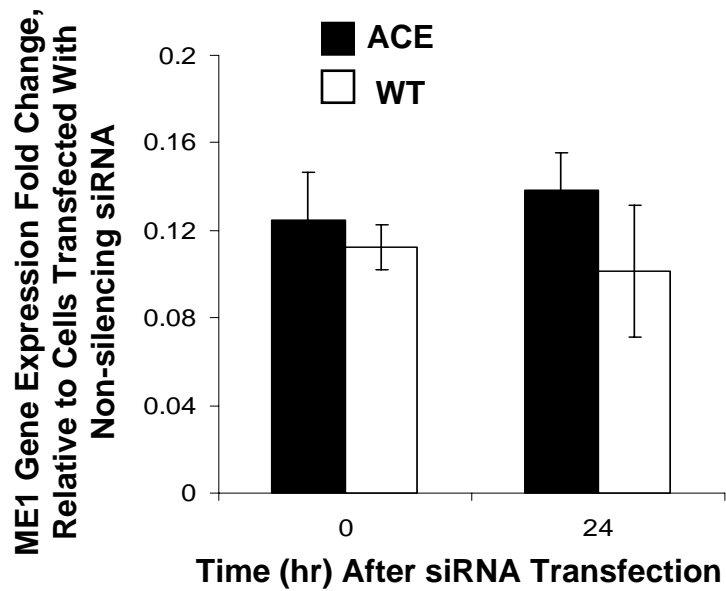


Figure S3. Malic Enzyme 1 (ME1) levels over time after knockdown of ME1 using siRNA as described in Methods. Fatty acid uptake assay was started at time zero and continued for 24 hours. ME1 was knocked down nearly 90% for the duration of the experiment. Mean \pm SEM; n = 3.

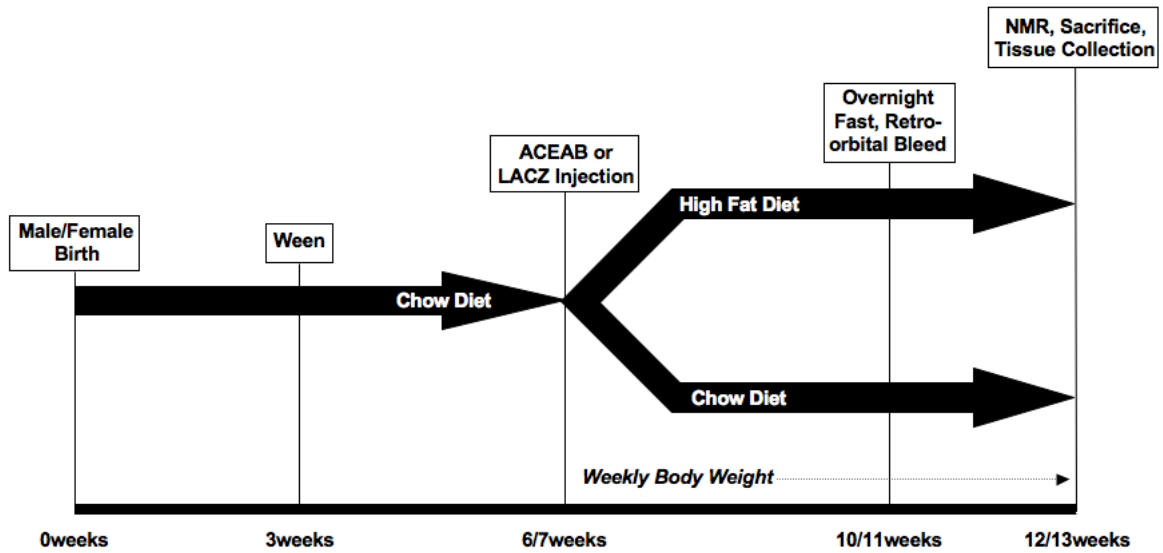


Figure S4. Experimental Protocol-1 for mouse experiments. Mice were weaned at 3 weeks and fed a standard chow diet until 6 weeks of age. At six weeks of age, mice were injected with either ACEAB or LACZ and placed on a standard chow or high fat diet. For 6 weeks mice were housed in cages of 1-4 and body weight was measured weekly. At 10/11 weeks of age mice (12/13 weeks for males) were fasted overnight and blood was collected via retro-orbital bleed. Six weeks post injection mice analyzed with NMR and sacrificed.

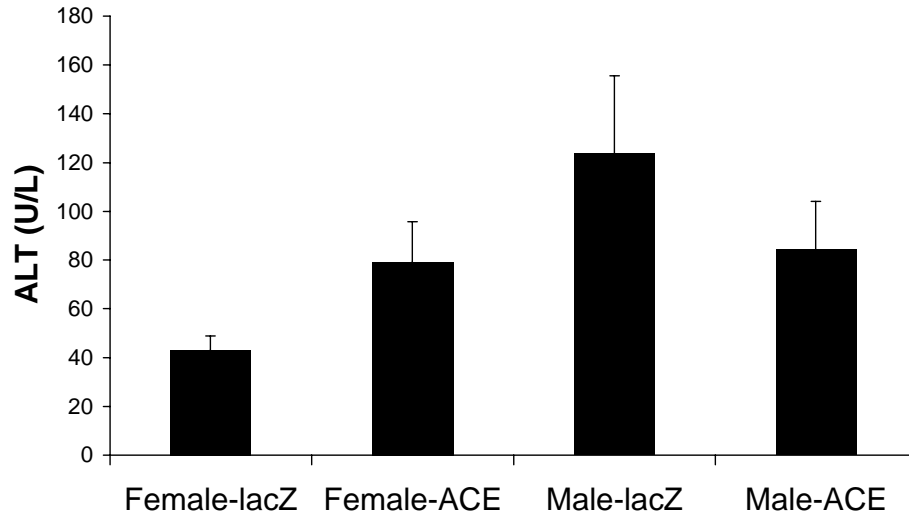


Figure S5. Alanine aminotransferase (ALT) serum levels were measured four weeks after tail vein injection of plasmid DNA. Mean \pm SEM; n = 4-5.

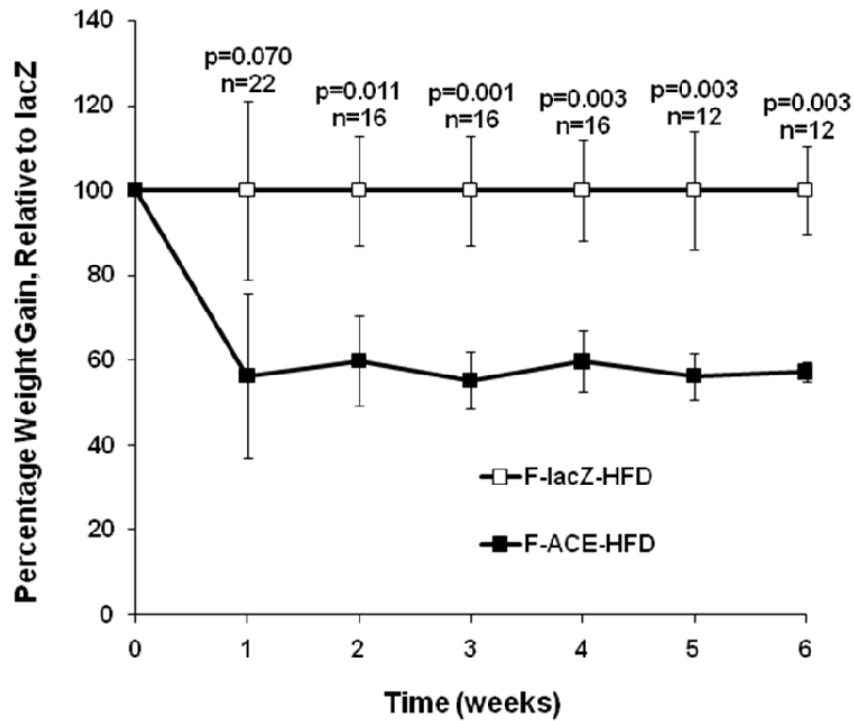


Figure S6. Percentage weight gain relative to F-lacZ mice for F-ACE and F-lacZ mice on HFD for 6 weeks. F-ACE mice gain less weight on HFD compared to F-lacZ. This figure includes weight gain data for 5 independent ACE and lacZ injection sets. Typically 3-6 mice were injected with lacZ or ACE per injection set. This normalization allows comparison of weight gain between different injection sets where litter size (Koopman et al., 1990; Roberts et al., 1988) was found to influence total weight gain. Mean \pm SEM

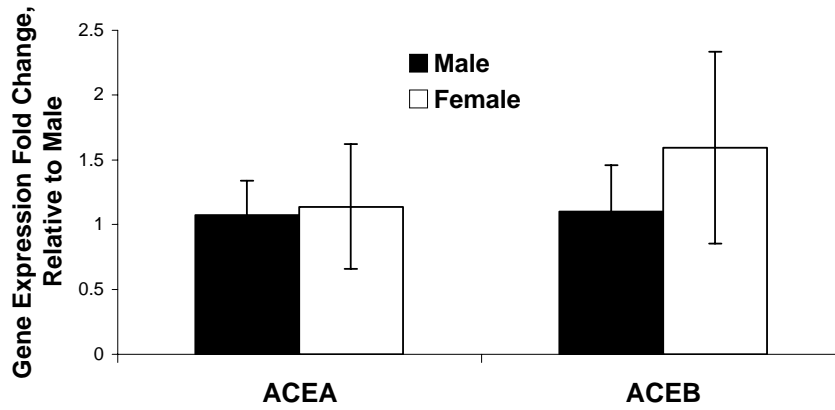


Figure S7. Isocitrate lyase (ACEA) and malate synthase (ACEB) gene expression levels between male and female ACE mice as determined by RT-PCR. Female mice expressing the glyoxylate shunt resist diet-induced obesity to a greater extent than male mice and this difference is not due to differences in transgene gene expression. Mean \pm SEM, n=3–4.

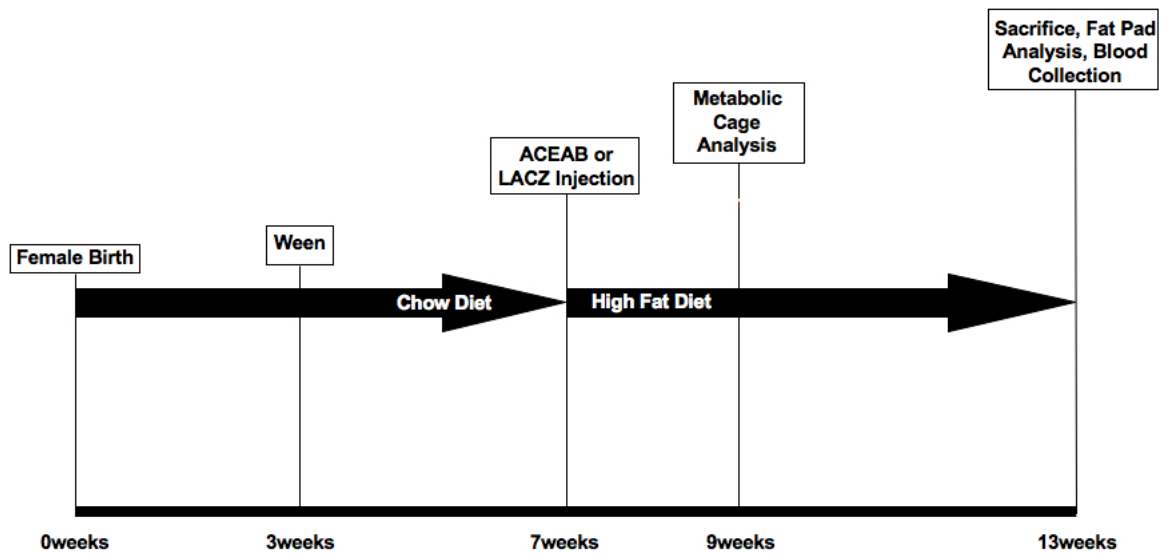


Figure S8. Experimental Protocol-2 for mouse experiments. Female mice were weaned at 3 weeks and fed a low fat chow diet until 6 weeks of age. At six weeks of age, mice were injected with either ACEAB or LACZ and placed on a high fat diet. Two weeks after injection mice were analyzed in metabolic cages. Six weeks post injection fat pads were analyzed, blood was collected after overnight fast, and mice were sacrificed.

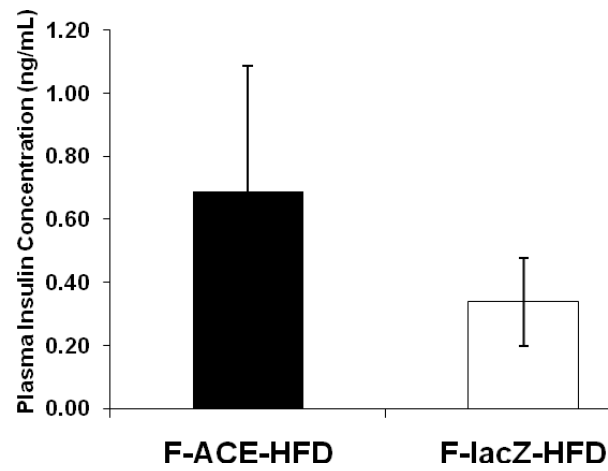


Figure S9. Fasting plasma insulin levels were measured in female ACE and lacZ injected mice after 6 weeks on HFD. F-ACE and F-lacZ were found to have similar plasma insulin concentrations. Mean \pm SEM; n = 3.

Supplemental Tables

Table S1: Metabolite abbreviations used for representation of glucose, fatty acid, and triglyceride metabolism and oxidative phosphorylation (Figure 3B).

Abbreviation	Full Name
Glucose_ext	Extracellular glucose
Glucose_int	Intracellular glucose
G6P	Glucose-6-phosphate
F6P	Fructose-6-phosphate
F-1,6-BP	Fructose-1,6-biphosphate
GAP	D-glyceraldehyde-3-phosphate
DHAP	Dihydroxy-acetone-phosphate
1,3-DPG	1,3-diphosphateglycerate
3PG	3-phosphoglycerate
2PG	2-phosphoglycerate
PEP	Phosphoenolpyruvate
PYR	Pyruvate
Acetyl-CoAm	Acetyl-Coenzyme A, mitochondria
Acetyl-CoAc	Acetyl-Coenzyme A, cytoplasm
LAC	Lactate
OAAc	Oxaloacetate, cytoplasm
OAAm	Oxaloacetate, mitochondria
MALm	Malate, mitochondria
MALc	Malate, cytoplasm
FUM	Fumarate
SUCC	Succinate
GLYX	Glyoxylate
a-KG	alpha-ketoglutarate
ICIT	Isocitrate
C-ACO	Cis-aconitate
CITc	Citrate, cytoplasm
CITm	Citrate, mitochondria
3-KA	3-ketoacyl coenzyme-A
L-3-H	L-3-hydroxyacyl coenzyme-A
T-EN	Trans-2-enoyl coenzyme-A
EN-CoA	Enoyl coenzyme-A
A-CoA	Acyl coenzyme A
FA-CoAm	Fatty acid coenzyme-A, mitochondria
FA-CRNm	Fatty acyl carnitine, mitochondria
FA-CRNc	Fatty acyl carnitine, cytoplasm
FA-CoAc	Fatty acid coenzyme-A, cytoplasm
FA	Fatty acid
NADH	Dihydrodiphosphopyridine nucleotide
GLY	Glycerol
G3P	Glycerol-3-phosphate
A-G3P	1-acyl-sn-glycerol-3-phosphate
LPHA	L-phosphatidate
DAG	Diacylglycerol

Table S2: Metabolic reactions from glycolysis, fatty acid beta-oxidation, and triglyceride synthesis. Expression levels of these genes, along with others, were analyzed using microarray to determine the global effect glyoxylate shunt implementation.

Precursor(s)	Product(s)	Abbreviation	Gene Name
Glucose_ext	Glucose_int	SLC2A1	solute carrier family 2 (facilitated glucose transporter), member 1
Glucose_ext	Glucose_int	SLC2A3	solute carrier family 2 (facilitated glucose transporter), member 3
Glucose_int	G6P	HK2	hexokinase 2
G6P	F6P	GPI	glucose-6-phosphate isomerase
F6P	F-1,6-BP	PFK	6-phosphofructo-2-kinase/fructose-2,6-biphosphatase 2
F-1,6-BP	DHAP, GAP	ALDOC	aldolase C, fructose-bisphosphate
DHAP	GAP	TPI1	triosephosphate isomerase
GAP	1,3-DPG	GAPD	glyceraldehyde-3-phosphate dehydrogenase
1,3-DPG	3PG	PGK1	phosphoglycerate kinase 1
3PG	2PG	PGAM2	phosphoglycerate mutase
2PG	PEP	ENO3	enolase 3
PEP	PYR	PKLR	pyruvate kinase, liver
PYR	LAC	LDH	lactate dehydrogenase
PYR	ACETYL-COA	PDK1	pyruvate dehydrogenase kinase, isoenzyme 1
PYR	OAAm	PC	pyruvate carboxylase
ACETYL-COAm,	CITm	CS	citrate synthase
OAA	C-ACO	ACO2	aconitate hydratase
CITm	ICIT	ACO1	aconitase 1
C-ACO	GLYX, SUCC	ACEB	Malate synthase
ICIT	a-KG	IDH3A	isocitrate dehydrogenase 3 (NAD+) alpha
ICIT	SUCC	SUCLA2	Succinyl coenzyme-A ligase
a-KG	FUM	SDHA	succinate dehydrogenase
SUCC	MALm	FH	fumarate hydratase
FUM	OAAm	MDH2	malate dehydrogenase
M\AIm	MALm	ACEA	Isocitrate lyase
ACETYL-COAm,	FA	ACSL1	acyl-CoA synthetase long-chain family member 1
GLYX	FA-COAc	CPT1A	carnitine palmitoyltransferase 1A (liver)
FA	FA-CRNc	CRAT	carnitine acetyltransferase
FA-COAc	FA-CRNm	CPT2	carnitine palmitoyltransferase 2
FA-CRNc	FA-COAm	FACL3	Acyl-CoA synthetase long-chain family member 3
FA-CRNm	A-COA	ACADM	acyl-coa dehydrogenase
FA-COAm	EN-COA	PECI	Peroxisomal 3,2-trans-enoyl-coa isomerase
A-COA	TEN	HADHA	trifunctional enzyme alpha-subunit
EN-COA	L-3-H	HADH2	hydroxyacyl-Coenzyme A dehydrogenase, type II
A-COA	3-KA	ACAA2	3-ketoacyl coenzyme-A thiolase
TEN	ACETYL-COAm	GK	glycerol kinase
L-3-H	G3P	GPAT	glycerol-3-phosphate acyltransferase
3-KA	A-G3P	GNPAT	glyceronephosphate O-acyltransferase
GLY	LPHA	PPAP2B	phosphatidic acid phosphatase type 2B
G3P	DAG	DGAT	diacylglycerol o-acyltransferase
A-G3P	TG		
LPHA			
DAG			

CITc	ACETYL-COAc, OAAc	ACLY	ATP citrate lyase
ACETYL-COAc	MALONYL-COA	ACC	Acetyl-Coenzyme-A carboxylase
MALc	MALm	SLC25A10	Dicarboxylate transporter
OAAc	PEP	PEPCK	Phosphoenolpyruvate carboxykinase

Table S3: Gene names, accession numbers, and fold changes of genes involved in glycolysis, fatty acid beta-oxidation, and triglyceride synthesis. Data was processed using dChip.

Gene Name	Accession	Fold Change	Lower Bound	Upper Bound
solute carrier family 2 (facilitated glucose transporter), member 1	NM_006516	-1.33	-1.23	-1.43
solute carrier family 2 (facilitated glucose transporter), member 3	AI631159	-2.91	-2.6	-3.24
hexokinase 2	AI761561	-1.21	-1.11	-1.32
glucose-6-phosphate isomerase	NM_000175	--	--	--
6-phosphofructo-2-kinase/fructose-2,6-biphosphatase 2	NM_006212	-1.41	-1.28	-1.54
aldolase C, fructose-bisphosphate triosephosphate isomerase	NM_005165	-2	-1.84	-2.18
glyceraldehyde-3-phosphate dehydrogenase	NM_000365	--	--	--
phosphoglycerate kinase 1	NM_002046	--	--	--
phosphoglycerate mutase	NM_000291	-1.27	-1.18	-1.37
enolase 3	NM_000290	--	--	--
pyruvate kinase, liver	NM_001976	-1.75	-1.47	-2.07
lactate dehydrogenase	NM_000298	--	--	--
pyruvate dehydrogenase kinase, isoenzyme 1	NM_005566	--	--	--
pyruvate carboxylase	NM_002610	-1.37	-1.14	-1.62
citrate synthase	NM_022172	-1.42	-1.21	-1.69
aconitate hydratase	NM_004077	--	--	--
aconitase 1	NM_001098	--	--	--
Malate synthase	NM_001098	--	--	--
isocitrate dehydrogenase 3 (NAD+) alpha	2.3.3.9	--	--	--
Succinyl coenzyme-A ligase	NM_005530	1.22	1.15	1.28
succinate dehydrogenase	NM_003850	--	--	--
fumarate hydratase	AI348006	-1.2	-1.11	-1.31
malate dehydrogenase	NM_000143	1.22	1.12	1.33
Isocitrate lyase	AAA39509	--	--	--
acyl-CoA synthetase long-chain family member 1	4.1.3.1	--	--	--
carnitine palmitoyltransferase 1A (liver)	NM_001995	1.64	1.41	1.95
carnitine acetyltransferase	BF001714	1.43	1.33	1.54
carnitine palmitoyltransferase 2	BC000723	1.24	1.14	1.36
Acyl-CoA synthetase long-chain family member 3	NM_000098	--	--	--
acyl-coa dehydrogenase	AL525798	1.43	1.35	1.53
Peroxisomal 3,2-trans-enoyl-coa isomerase	NM_000016	--	--	--
trifunctional enzyme alpha-subunit	CAG33049	--	--	--
hydroxyacyl-Coenzyme A dehydrogenase, type II	NM_000182	--	--	--
3-ketoacyl coenzyme-A thiolase	NM_004493	1.33	1.23	1.44
glycerol kinase	NM_006111	--	--	--
glycerol-3-phosphate acyltransferase	AJ252550	1.23	1.1	1.36
glyceronephosphate O-acyltransferase	2.3.1.15	--	--	--
phosphatidic acid phosphatase type 2B	NM_014236	-1.29	-1.23	-1.36
diacylglycerol o-acyltransferase	AB000889	-2.07	-1.67	-2.59
ATP citrate lyase	NM_012079	--	--	--
Acetyl-Coenzyme-A carboxylase	NM_001096	1.3	1.19	1.42
	S41121	--	--	--

Dicarboxylate transporter	NM_012140	--	--	--
Phosphoenolpyruvate carboxykinase	NM_004563	--	--	--

Supplementary Table 4: Figure 3B abbreviations, gene abbreviations, gene names, accession numbers, and fold change of genes involved in oxidative phosphorylation. Fatty acid beta-oxidation is closely linked to oxidative phosphorylation since it results in production of reducing equivalents.

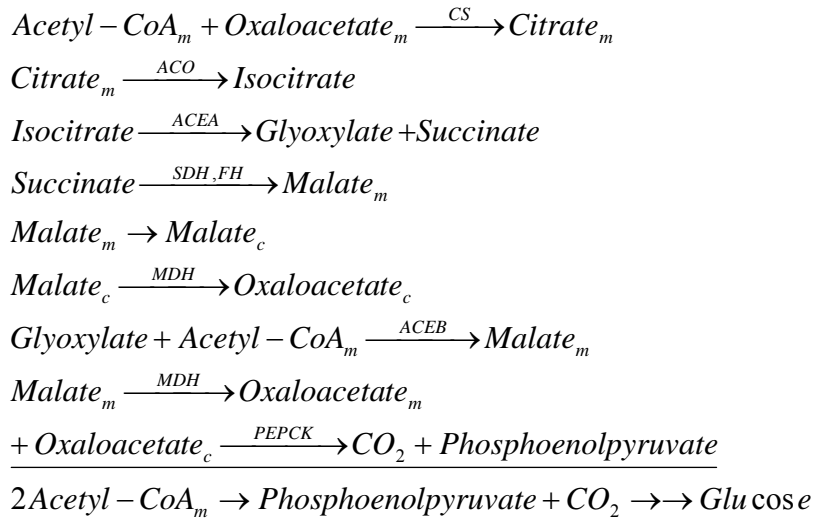
Figure Abbreviation	Abbreviation	Gene Name	Accession	Fold Change	Upper Bound	Lower Bound
I	NDUFA6	NADH dehydrogenase (ubiquinone) 1 alpha subcomplex, 6, 14kDa	BC002772	1.57	1.45	1.71
II	SDHA	succinate dehydrogenase	AI348006	-1.2	-1.11	-1.31
III	CYCS	cytochrome c, somatic	BC005299	1.49	1.38	1.62
IV	MTC01	Cytochrome oxidase	NM_173704	--	--	--
V	ATP6V0B	ATPase, H ⁺ transporting, lysosomal 21kDa, V0 subunit c" /// ATPase, H ⁺ transporting, lysosomal 21kDa, V0 subunit c"	BC005876	1.49	1.33	1.68
UCP2	UCP2	uncoupling protein 2 (mitochondrial, proton carrier)	U94592	2.38	1.86	3.27

Supplementary Table 5: RT-PCR verification of microarray analysis. RNA was extracted using RNeasy Columns (Qiagen) as described in Methods. Fold changes were calculated using the $\Delta \Delta C_t$ method with beta-actin as an endogenous control. Positive numbers indicated that the ACE cell line had higher expression levels than WT. Negative numbers indicate that the ACE cell line had lower expression levels.

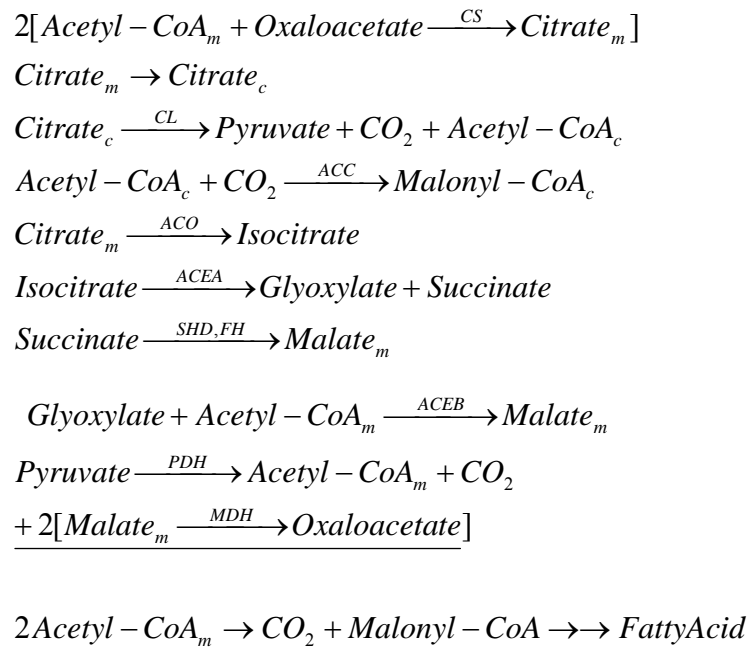
Gene Name	Forward Primer	Reverse Primer	Fold Change	SE
HK2	CAAAGTGACAGTGGGTGTGG	GCCAGGTCCTTCACTGTCTC	-1.290702844	0.086868
ALDOC	GGCTGCCACTGAGGAGTTC	CTGCTGCTCCACCATCTTCT	-2.380508363	0.347125
HAHD2	ATCAAACTGCCAGTGTGGCT	AGTGTGATGCCCACTATTCCC	1.619757928	0.172241
SLC2A3	CCAACTTCCTAGTCGGATTG	AGGAGGCACGACTTAGACAT	-1.909181666	0.036516
ACLS1	AGTCCCCTGTGGTTTCTGTTG	TTGCCAGAGGCTCCTTATCTG	2.063172255	0.307837
PC	CCAGAGGCAGGTCTTCTTTG	GGCCCTTACGTCCTTTAG	-1.224888027	0.083426

Supplemental Experimental Procedures

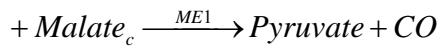
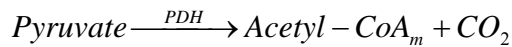
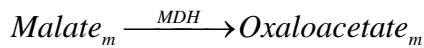
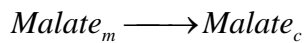
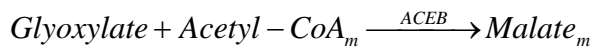
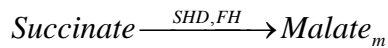
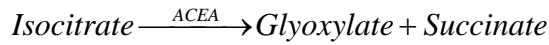
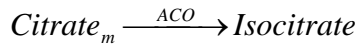
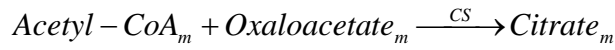
ACE1: Glyoxylate shunt for gluconeogenesis.



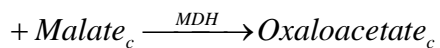
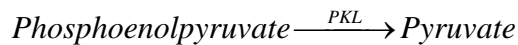
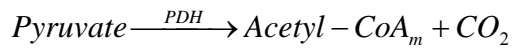
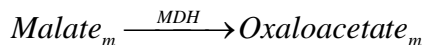
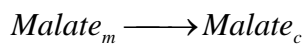
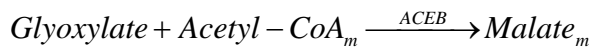
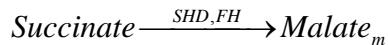
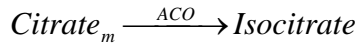
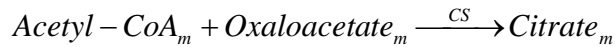
ACE2: Glyoxylate shunt for malonyl-CoA/fatty acid production.



ACE3: Glyoxylate shunt for complete acetyl-CoA oxidation through ME1.



ACE4: Glyoxylate shunt for complete acetyl-CoA oxidation through PEPCK.



This analysis can also be carried out using convex analysis(Liao et al., 1996) or extreme pathway analysis(Schilling et al., 2000).

Plasmid Construction. Isocitrate lyase (ACEA) and malate synthase (ACEB) were amplified by PCR using PFU polymerase (Stratagene, La Jolla, CA) from *Escherichia coli* strain BW25113 genomic DNA with primer sets 5'-AAAGCCAAGATCCATTCGTTGAAAACCCGT (containing 18nt from 3' end of MLS) and reverse primer 5'-CCAGATCTGAACTGCGATTCTTCAGT (containing an engineered *Bgl* II site), and 5'-AAAGCCAAGATCCATTCGTTGACTGAACAGGCAACAAC (containing 18nt from 3' end of MLS) and reverse primer 5'-CCCTCTAGACGATAACAGGCGGTAGCCTGG (containing an engineered *Xba* I site) respectively. To direct ACEA and ACEB to the mitochondria, a mitochondria leader sequence (MLS) was PCR amplified from pCMV/*myc*/mito (Invitrogen, Carlsbad, CA) with forward primer 5'-ACGTGGTGCGGCCGCATGTCCGTCCT (containing an engineered *Not* I site) for ACEA and 5'-CCCAAGCTTGATGTCCGTCCTGACGC (containing an engineered *Hind* III) site for ACEB. The MLS and corresponding genes were combined in frame by splicing by overlap extension (SOE) (Horton et al., 1989), creating MLS-aceA and MLS-aceB fragments. MLS-aceA PCR fragment was cloned into the pBudCE4.1 (Invitrogen, Carlsbad, CA) *Not* I-*Bgl* II sites, in frame with a V5 epitope. MLS-aceB PCR fragment was cloned into the *Hind* III-*Xba* I sites, in frame with a *myc* epitope. The resulting vector containing both genes was designated pBudaceAB. For mouse studies, MLS-aceA and MLS-aceB were cloned from pBudaceAB into pLIVE vector (Mirus Bio, Madison, WI). MLS-aceA was PCR amplified using forward primer 5'-GGGGCTAGCATGTCCGTCCTGACGCC (containing an engineered *Nhe* I site) and reverse primer 5'-

GGGCTCGAGAGTCGAGGCTGATCAGCG (containing an engineered *Xho I* site).
MLS-aceB was PCR amplified using forward primer 5'-GGG
GCTAGCATGTCCGTCCTGACGCC (containing an engineered *Nhe I* site) and reverse
primer 5'-GGGCTCGAGTCATGTCTGAATTCCCGGG (containing an engineered *Xho I*
I site). These vectors were designated pLIVE-A and pLIVE-B, respectively.

Cell Culture. Human hepatoma cell line, HepG2 (American Type Culture Collection) was maintained in DMEM supplemented with 10% heat-inactivated FBS and 50ug/mL penicillin, 50ug/mL streptomycin, and 100ug/mL neomycin at 37°C in a humidified atmosphere containing 5% CO₂. Cells were transfected in 60mm plates with pBudaceAB or pBudCE4.1 with Lipofectamine 2000 (Invitrogen, Carlsbad, CA) according to manufacturer's protocols. 24 hours after transfection, cells were transferred to a 15cm diameter plate in DMEM media supplemented with 320ug/mL Zeocin (Invitrogen, Carlsbad, CA). Fresh media was supplied every three days and after 6 weeks colonies were isolated, propagated, and the presence of MLS-ACEA and MLS-ACEB was determined by reverse-transcriptase PCR. For reverse transcriptase PCR, total RNA was extracted from 60mm cell culture plates using RNeasy plus columns (Qiagen, Valencia, CA). For detection of MLS-ACEA, 5'-ACGTGGTGCGGCCGCATGTCCGTCCT and 5' – CCAGATCTGAACTGCGATTCTTCAGT were used for forward and reverse primers, respectively. For detection of MLS-ACEB, 5'-CCCAAGCTTGATGTCCGTCCTGACGC and 5'-CCCTCTAGACGATAACAGGCGGTAGCCTGG were used for forward and reverse

primers, respectively. Reverse transcriptase reactions were performed using the Smart MMLV Reverse Transcriptase kit (Clontech, Mountain View, CA). Isocitrate lyase (Chell et al., 1978) and malate synthase (Sundaram et al., 1980) enzyme activity was assayed spectroscopically.

Metabolite Analysis. 16 hours prior to fatty acid uptake assays cells were seeded 1.75×10^5 cells/well in 24-well multi plates containing DMEM supplemented with 10%FBS. Cells were washed with PBS and then incubated in 1.5mL of DMEM media enriched with palmitate at various concentrations. Four 50uL samples of media were taken over a 24 hour period and stored at -20°C for further analysis. After 24 hours, medium was aspirated and total protein was assayed by the method of Bradford (Bradford, 1976). Metabolites were quantified using high performance liquid chromatography (HPLC) on an Agilent 1100 model (Agilent Technologies, Palo Alto, CA) consisting of a binary pump, autosampler, and degasser connected to an organic acid Aminex HPX-87H column (300x7.8mm, Bio-Rad). A mobile phase of 5mM sulfuric acid was used and the column was maintained at 65°C with a flowrate of 0.6mL/min. Lactate and other organic acids were quantified with a diode array detector (Agilent Technologies) at wavelengths of 210nm and 254nm. Glucose and other non-UV absorbing compounds were quantified using a refractive index detector (Agilent Technologies). Standard curves were prepared before each set of samples was analyzed. Concentration profiles were normalized to the total amount of protein or cell number.

Gluconeogenesis Assay. Gluconeogenesis was assed as previously described (Zhou et al., 2005) with minor modifications. Sixteen hours prior to the assay 3×10^5 cells/well were transferred to 24-well plates. To measure gluconeogenesis, cells were washed 3X with PBS and incubated 4 hours in 250uL glucose production medium consisting of glucose free DMEM with either 200uM [U- ^{13}C] palmitate + 2% free fatty acid free BSA, 20mM [U- ^{13}C] glycerol, or no gluconeogenic substrate. Glucose concentration in the medium was then quantified using HPLC and ^{13}C enrichment was determined by converting glucose to pentacetate derivative (Tserng and Kalhan, 1983) and GC-MS analysis (Sriram et al., 2008). Glucose carbons 2-6, m/z 98 in the mass spectrum (Tserng and Kalhan, 1983) after electron ionization, were analyzed in the selected ion monitoring mode.

Fatty Acid Fluorescence Uptake Assay. Fatty acid fluorescence uptake assays were performed using QBT FA Uptake Assay (Liao et al., 2005) according to manufacturer's protocols with minor modifications (Molecular Devices, Sunnyvale, CA) and imaged as previously described (Fung et al., 2005). Assays were performed using 8-well chambered coverglass culture dishes (Lab-Tek, Rochester, NY) with flat glass bottoms. ACE and WT cells were seeded 90% confluent (1.27×10^5 cells/well) the night before assay was to be performed. All loading buffers were prepared exactly as recommended by manufacturer. On the day of the assay, medium was aspirated and cells were incubated in 333uL serum free DMEM medium for 1 hour. After serum starving, 333uL loading buffer was added to each well and fluorescence was monitored.

¹⁴CO₂ Production from [U-¹⁴C] Palmitate. Production of ¹⁴CO₂ was measured as previously described (Harwood et al., 2003) using [U-¹⁴C] palmitate. On the day of the study, cells were washed twice with PBS and incubated in trypsin-EDTA for 5min to detach cells from plates. Cells were resuspended in suspension buffer composed of Krebs bicarbonate buffer consisting of 3mM glucose, 10mM HEPES, and 2% fatty acid free BSA to a concentration of 1.5*10⁷cells/ml. 2mL of cell suspensions were added to 25mL Erlenmeyer-Konte flasks fitted with a center well and incubated at 37°C for 30min. After incubation, a 0.5ml aliquot of suspension buffer containing 3.0μCi of [U-¹⁴C] palmitate (Amersham Biosciences, Piscataway, NJ) was added and the flasks were incubated for 2hr at 37°C with shaking. The reaction was terminated by addition of 0.5mL of 0.5M H₂SO₄. ¹⁴CO₂ was collected by addition of 300uL 1M benzethonium hydroxide to the center well and incubating at 37°C for 2hours or at room temperature overnight. After incubation, the center well was removed and added to a scintillation vial containing 6mL scintillation cocktail and counted on a liquid scintillation counter.

siRNA Knockdown of Malic Enzyme. Malic enzyme 1 knockdown was performed using a RNAi Human Starter Kit (Qiagen, Valencia, CA) and the following siRNA duplex: r(GAA CAA AUU CUC AAA GAU A)d(TT). The day before transfection, ACE and WT cells were seeded at a density of 60,000 cells/well in 24-well plates containing 0.5mL DMEM growth medium. The day of transfection, 37.5ng siRNA was diluted in 100uL serum free DMEM to give a final siRNA concentration 5nM. Next, 3uL of HiPerFect (Qiagen, Valencia, CA) transfection reagent was added to the diluted siRNA and the solution was mixed by vortexing. The samples were incubated at room

temperature for approximately 10min to allow the formation of transfection complexes. After incubation, the complexes were added drop-wise to the cells. After 48 hours, either metabolic analysis (DMEM + 300uM palmitate) was performed or total RNA was harvested for quantification to verify knockdown. Quantitative RT-PCR was performed using SYBR Green chemistry and Smart Cyclers (Cepheid, Sunnyvale, CA) and fold changes were calculated using $\Delta\Delta C_t$ method with beta-actin as an endogenous control. Primer sets were Quantitect Primer assays (Qiagen, Valencia, CA). Transfection of a non-silencing fluorescent siRNA had no effect on phenotype.

Real-Time PCR. For real-time pcr (RT-PCR) analysis, total RNA was isolated using RNeasy-plus columns (Qiagen, Valencia, CA). First strand cDNA was synthesized using either 2-3ug (HepG2) or 500ng (mouse) of RNA and Superscript III Reverse Transcriptase (Invitrogen, Carlsbad, CA). Quantitative RT-PCR was performed using SYBR Green chemistry, Quantitect Primer Assays (Qiagen, Valencia, CA), and Smart Cyclers (Cepheid, Sunnyvale, CA) and fold changes were calculated using $\Delta\Delta C_t$ method (Livak and Schmittgen, 2001) with beta-actin as an endogenous control.

Microarray Expression Analysis. Isolated total RNA samples were processed as recommended by Affymetrix, Inc. (Affymetrix GeneChip[®] Expression Analysis Technical Manual, Affymetrix, Inc., Santa Clara, CA). In brief, total RNA was initially isolated using Trizol Reagent (Gibco BRL Life Technologies, Rockville, MD), and passed through an RNeasy spin column (Qiagen, Valencia, CA) for further clean up. Eluted total RNA was quantified with a portion of the recovered total RNA adjusted to a

final concentration of 1.25ug/ul. All starting total RNA samples were quality assessed prior to beginning target preparation/processing steps by running out a small amount of each sample (typically 25-250ng/well) onto a RNA Lab-On-A-Chip (Caliper Technologies Corp., Mountain View, CA) that was evaluated on an Agilent Bioanalyzer 2100 (Agilent Technologies, Palo Alto, CA). Single-stranded, then double-stranded cDNA was synthesized from the poly(A)+ mRNA present in the isolated total RNA (typically 10 ug total RNA starting material each sample reaction) using the SuperScript Double-Stranded cDNA Synthesis Kit (Invitrogen, Carlsbad, CA) and poly (T)-nucleotide primers that contained a sequence recognized by T7 RNA polymerase. A portion of the resulting ds cDNA was used as a template to generate biotin-tagged cRNA from an *in vitro* transcription reaction (IVT), using the Affymetrix GeneChip® IVT Labeling Kit. In either case, 15ug of the resulting biotin-tagged cRNA was fragmented to an average strand length of 100 bases (range 35-200 bases) following prescribed protocols (Affymetrix GeneChip® Expression Analysis Technical Manual). Subsequently, 10ug of this fragmented target cRNA was hybridized at 45°C with rotation for 16 hours (Affymetrix GeneChip® Hybridization Oven 640) to probe sets present on an Affymetrix HGU-133A_2 array. The GeneChip® arrays were washed and then stained (SAPE, streptavidin-phycoerythrin) on an Affymetrix Fluidics Station 450, followed by scanning on a GeneChip® Scanner 3000. The results were normalized using GCOS 1.2 software using default values. For normalization, 'All Probe Sets Normalization' was used. This normalizes the average signal of the experiment to the average signal of the baseline. The results were quantified and analyzed using GCOS 1.2 software (Affymetrix, Inc.) using default values (Scaling, Target Signal Intensity = 500;

Normalization, All Probe Sets; Parameters, all set at default values). Expression fold changes were calculated using dChip software (Zhong et al, Nucleic Acids Research 31: 3483, 2003) and results were filtered using a 90% confidence bound of fold change. Expression changes were verified using RT-PCR. Our data was submitted to the NCBI Gene Expression Omnibus in MIAME format with access number GSE5903. The data can be accessed at:

<http://www.ncbi.nlm.nih.gov/geo/query/acc.cgi?token=tzqrpeciomgaqzy&acc=GSE5903>

Western Blotting. To determine the expression of MLS-ACEA and MLS-ACEB, proteins were extracted and concentration was determined as previously described (Bradford, 1976). Twenty micrograms of protein were separated on a 7.5% Tris-HCl SDS-PAGE gel and electroblotted onto polyvinylidene difluoride membranes (Bio-Rad, Hercules, CA) overnight at 4°C using standard methods. The membranes were blocked in 0.01M PBS, 0.05% Tween 20 buffer (PBST) containing 5% blotto for 1 hour at room temperature. To detect MLS-aceA, the membranes were incubated with anti-V5-HRP (1:1000) (Invitrogen, Carlsbad, CA) for 2.5 hours. For MLS-aceB detection, the membrane was incubated with anti-*myc*-HRP (1:5000) (Invitrogen, Carlsbad, CA) for 2 hours. The membranes were washed for 30min in PBST and developed using an ELC-plus kit (Amersham Biosciences, Piscataway, NJ). For time course experiments, ACE and WT cells were given DMEM supplemented with 300uM palmitate and protein was harvested at various time points over 24 hours. These proteins were detected in a similar manner, with the following exceptions: primary antibody incubation was overnight at 1:1000 dilution at 4°C and secondary antibody incubation was at 1:10000 dilution for

1 hour at room temperature. Antibodies were from Invitrogen and Cell Signaling (Danvers, MA).

Animal Care. All animal procedures and care were within institutional ARC guidelines. Male and female C57BL/6 mice (Taconic, Hudson, NY) were housed in cages of 1-4 at 22-24°C with a 12 hour light/dark cycle with food and water provided ad libitum. Until 6-7 weeks of age, all animals received a low fat chow diet (PicoLab Rodent Diet 20, 4.07 Kcal/g, 24.7% calories from protein, 13.2% from fat, and 62.1% carbohydrate). From 6-7 weeks of age, animals either received a low fat chow diet or high fat diet (Research Diets D12492, 5.24 Kcal/g, 20% calories from protein, 60% from fat, and 20% from carbohydrate).

Tail Vein Injections. Six to seven week old male and female mice (18-24g) were tail vein injected (Alino et al., 2003; Bates et al., 2006; Huang et al., 2006) with either pLIVE-A (20ug) and pLIVE-B (20ug) or pLIVE-lacZ (10ug) using the *TransIT In Vivo* Gene Delivery System (Mirus Bio, Madison, WI) as described in manufacture's protocol (<http://www.mirusbio.com/pdf/ML005.pdf>). All plasmids for injections (pLIVE-A, pLIVE-B, pLIVE-lacZ) were prepared using an EndoFree Plasmid Maxi Kit (Qiagen, Valencia, CA). Plasmids pLIVE-A and pLIVE-B were adjusted to a concentration of 2mg/mL and pLIVE-lacZ to 1mg/mL. For injection of pLIVE-A and pLIVE-B, 10uL of each plasmid was mixed with 160uL sterile endotoxin free water and 20uL *TransIT In Vivo* Polymer solution. The solution was vortexed for 5 seconds, incubated at room temperature for 5 minutes, and mixed with 1.9mL *TransIT In Vivo* Delivery Solution.

The entire solution was immediately injected with a 27-gauge needle into the tail vein within 7 seconds. For pLIVE-lacZ injections, the same procedure was followed with the following exceptions: 10uL of the plasmid was mixed with 180uL sterile endotoxin free water and 10uL *TransIT In Vivo* Polymer solution.

Experimental Protocol-1. Immediately after injection, male and female mice were placed on either a chow diet or high fat diet. For 6 weeks, body weight was measured weekly. At the end of four weeks, blood from females was collected via retro-orbital bleed after an overnight fast and stored at -80°C until further analysis(Castellani et al., 2008) (blood from males was collected in similar fashion after 6 weeks). Six weeks post-injection fat and lean mass was determined with a mouse Minispec (Brucker Woodlands, TX) and data was analyzed with software from Echo Medical Systems (Houston, TX) as previously described(Estrada-Smith et al., 2006). Animals were then sacrificed by cervical dislocation and liver, kidney, and lung were immediately flash-frozen in liquid nitrogen and stored at -80°C. To verify transgene expression, ~40mg of tissue was homogenized with a rotor stator homogenizer and RNA was extracted using RNeasy-plus columns (Qiagen, Valencia, CA).). First strand cDNA was synthesized with Superscript III Reverse Transcriptase (Invitrogen, Carlsbad, CA). The resulting cDNA was used at PCR template with the following primers: 5'-TCAGTGAAGAAATGCGGTCA and 5'-GCCGGTAATAAATTCGCTGT for MLS-ACEA and 5'-CGAGCAGGAGAAGCAAATTC and 5'-GCGAATTTTCCAATCAGCAT for MLS-ACEB. Beta-actin primers were from Qiagen.

Experimental Protocol-2. . Immediately after injection, female mice were placed on a high fat diet and two weeks after injection mice were analyzed in metabolic cages. Six weeks post-injection blood was collected after overnight fast and visceral fat pads were removed and weighed.

Malonyl-CoA Assay. Hepatic malonyl-CoA from tissue was measured as described by McGarry *et al* (McGarry et al., 1978) with minor modifications. Acid soluble metabolites were extracted from ~10mg frozen tissue by homogenization in 0.5mL 6% (w/v) HClO₄. After 10 minute incubation on ice the homogenates were centrifuged at 5000g for 15 minutes at 4°C and the supernatant was collected. The extracts were neutralized to pH 7.0 with 3.5M KOH/1M K₂HPO₄ (~90uL), incubated on ice for 15 minutes to allow formation of KClO₄ precipitate, and centrifuged at 2000g for 15 minutes at 4°C. The resulting supernatant was used for malonyl-CoA assay. To assay for malonyl-CoA, 300uL of reaction mixture containing 0.2M KH₂PO₄ pH 7.0, 2.5mM dithiothreitol, 2mM EDTA, 0.2mM NADPH, 1mg/mL fatty acid-free BSA, 2nmol [1-¹⁴C] acetyl coA and 30uL liver extract or appropriate quantity of malonyl-CoA standard was added to a glass test tube. Tissue extracts with 0.2nmol malonyl-CoA added were run in parallel to account for unlabeled acetyl-CoA dilution. The reaction was initiated by addition of 4.5ug of purified fatty acid synthase and the tubes were covered with parafilm and incubated at 37°C for 3 hours. The reactions were terminated by adding 7.5uL 70% (w/v) HClO₄. To extract palmitate, 300uL of ethanol followed by 1.5mL petroleum ether was added and the tubes were vortexed for 10 seconds to aid phase separation. After separation, 1.2mL of petroleum ether phase was transferred to a second

glass tube containing 0.6mL water. The tubes were shaken and 1.0mL of the petroleum ether phase was transferred to a scintillation vial, dried under nitrogen, and counted with 6mL scintillation fluid. Blanks containing no malonyl-CoA were run in parallel and subtracted from sample values.

Leptin and Insulin Measurements. Leptin and Insulin were measured using ELISA (Crystal Chem, Downers Grove, IL).

Liver ATP. Liver total ATP was measured as described (Evans et al., 2008) with modifications using a bioluminescence based Eliten ATP Assay System (Promega, Madison, WI). Approximately 50mg of frozen tissue was homogenized in 500uL ice-cold homogenization buffer (20mM Tris pH =7.5, 150mM NaCl, 1.0% Triton X-100, 10% glycerol, 2mM EDTA, and complete protease inhibitor). A sample (50uL) of homogenate was saved for protein assay to normalize between samples. The remaining homogenate was acidified with 67.5uL of a 10% trichloroacetic acid solution and then centrifuged at max speed for 5 minutes. After centrifugation, 200uL of sample was transferred to a new tube and adjusted to pH=7.75 with 3M KOH/1M K₂HPO₄. The sample was then diluted 1:100 in 0.1mM Tris-Acetate pH=7.75 and 10uL of diluted sample was transferred to a 96 well plate. Bioluminescence was immediately measured in a luminometer using the Enlinter ATP assay system.

Liver Triglyceride Content. Liver TG content was measured using a triglyceride determination kit (Wako Diagnostics, Richmond, VA). Approximately 200mg of tissue

was homogenized in 500uL homogenization buffer (10mM Tris-HCl pH=7.4, 10mM NaCl, 1mM EDTA, 0.5% Triton X-100). After homogenization, 173uL of homogenate was mixed with 28uL of 20% Triton X-100 and the sample was vortexed for 2-4sec and centrifuged at 6000rpm for 1min at RT. The supernatant was transferred to a new tube after homogenization of the lipid partition and the TG content was measured using a triglyceride determination kit. Samples were normalized according to protein amount.

Indirect Calorimetry, Feeding and Activity. Animals were housed individually in a series of eight, airtight chambers designed to assess the metabolic activity of mice over three 12 hr light / 12 hr dark cycles (Oxymax, Columbus Instruments, OH). A standard gas mixture of O₂, CO₂, and N₂ was used to calibrate the system before each experiment. Animals were acclimated to the chambers over the first 24 hours and data was collected over the subsequent 48 hours. Mice were analyzed in two sets (eight mice per set, four per virus injected) in individual calorimeter chambers maintained at constant temperature and humidity. The mice had free access to water and powdered food presented from a food hopper attached to a scale. The volume of water intake and the weight of food consumed was recorded electronically. Room air gas was infused into each chamber at a set rate and every 15 minutes, both O₂ and CO₂ concentrations were measured in each chamber. The rate of oxygen consumption (VO₂) and carbon dioxide production (VCO₂) were calculated and averaged over the entire period as well as for the light and dark cycle for each mouse. In order to compare animals of different sizes, the consumption (VO₂) and production (VCO₂) values are normalized with respect to body weight and corrected according to a metabolically effective mass value (0.75) using the following equations:

$$\text{Normalized VO}_2 = \text{VO}_{2(\text{measured})} / [\text{weight (g)} / 1000 \text{ (g/kg)}]^{(\text{effective mass} = 0.75)}$$

$$\text{Normalized VCO}_2 = \text{VCO}_{2(\text{measured})} / [\text{weight (g)} / 1000 \text{ (g/kg)}]^{(\text{effective mass} = 0.75)}$$

The respiratory exchange ratio (RER) is simply the ratio of $\text{VCO}_2 / \text{VO}_2$ and is unitless. It is calculated from the measured VO_2 and VCO_2 prior to weight normalization or effective mass correction. The RER provides a relative measure of the total body metabolic pathways being used. An RER of 1.00 corresponds to “pure” carbohydrate consumption (100% of total O_2 consumed by metabolism of carbohydrate, 0% from fat), while an RER of 0.70 represents “pure” fatty acid oxidation (100% of total O_2 consumed by metabolism of fat, 0% from carbohydrate).

Supplemental References

Alino, S.F., Crespo, A., and Dasi, F. (2003). Long-term therapeutic levels of human alpha-1 antitrypsin in plasma after hydrodynamic injection of nonviral DNA. *Gene Ther* 10, 1672-1679.

Bates, M.K., Zhang, G., Sebestyen, M.G., Neal, Z.C., Wolff, J.A., and Herweijer, H. (2006). Genetic immunization for antibody generation in research animals by intravenous delivery of plasmid DNA. *Biotechniques* 40, 199-208.

Bradford, M.M. (1976). A rapid and sensitive method for the quantitation of microgram quantities of protein utilizing the principle of protein-dye binding. *Anal Biochem* 72, 248-254.

Castellani, L.W., Nguyen, C.N., Charugundla, S., Weinstein, M.M., Doan, C.X., Blaner, W.S., Wongsiriroj, N., and Lusic, A.J. (2008). Apolipoprotein AII is a regulator of very low density lipoprotein metabolism and insulin resistance. *J Biol Chem* 283, 11633-11644.

Chell, R.M., Sundaram, T.K., and Wilkinson, A.E. (1978). Isolation and characterization of isocitrate lyase from a thermophilic *Bacillus* sp. *The Biochemical journal* 173, 165-177.

Estrada-Smith, D., Collins, A.R., Wang, X., Crockett, C., Castellani, L., Lusic, A.J., and Davis, R.C. (2006). Impact of chromosome 2 obesity loci on cardiovascular complications of insulin resistance in LDL receptor-deficient C57BL/6 mice. *Diabetes* 55, 2265-2271.

Evans, Z.P., Ellett, J.D., Schmidt, M.G., Schnellmann, R.G., and Chavin, K.D. (2008). Mitochondrial uncoupling protein-2 mediates steatotic liver injury following ischemia/reperfusion. *J Biol Chem* 283, 8573-8579.

Fung, E., Wong, W.W., Suen, J.K., Bulter, T., Lee, S.G., and Liao, J.C. (2005). A synthetic gene-metabolic oscillator. *Nature* 435, 118-122.

Harwood, H.J., Jr., Petras, S.F., Shelly, L.D., Zaccaro, L.M., Perry, D.A., Makowski, M.R., Hargrove, D.M., Martin, K.A., Tracey, W.R., Chapman, J.G., *et al.* (2003). Isozyme-nonselective N-substituted bipiperidylcarboxamide acetyl-CoA carboxylase inhibitors reduce tissue malonyl-CoA concentrations, inhibit fatty acid synthesis, and increase fatty acid oxidation in cultured cells and in experimental animals. *J Biol Chem* 278, 37099-37111.

Horton, R.M., Hunt, H.D., Ho, S.N., Pullen, J.K., and Pease, L.R. (1989). Engineering hybrid genes without the use of restriction enzymes: gene splicing by overlap extension. *Gene* 77, 61-68.

- Huang, L.R., Wu, H.L., Chen, P.J., and Chen, D.S. (2006). An immunocompetent mouse model for the tolerance of human chronic hepatitis B virus infection. *Proc Natl Acad Sci U S A* *103*, 17862-17867.
- Koopman, J.P., Scholten, P.M., Van Den Brink, M.E., and Beynen, A.C. (1990). Availability of solid feed and growth rates of pre-weaned mice of different litter size. *Zeitschrift fur Versuchstierkunde* *33*, 217-219.
- Liao, J., Sportsman, R., Harris, J., and Stahl, A. (2005). Real-time quantification of fatty acid uptake using a novel fluorescence assay. *J Lipid Res* *46*, 597-602.
- Liao, J.C., Hou, S.-Y., and Chao, Y. (1996). Pathway Analysis, Engineering, and Physiological Considerations for Redirecting Central Metabolism. *Biotechnology and Bioengineering* *52*, 129-140.
- Livak, K.J., and Schmittgen, T.D. (2001). Analysis of relative gene expression data using real-time quantitative PCR and the 2^{(-Delta Delta C(T))} Method. *Methods (San Diego, Calif)* *25*, 402-408.
- McGarry, J.D., Stark, M.J., and Foster, D.W. (1978). Hepatic malonyl-CoA levels of fed, fasted and diabetic rats as measured using a simple radioisotopic assay. *J Biol Chem* *253*, 8291-8293.
- Roberts, J.L., Whittington, F.M., and Enser, M. (1988). Effects of litter size and subsequent gold-thioglucoase-induced obesity on adipose tissue weight, distribution and cellularity in male and female mice: an age study. *The British journal of nutrition* *59*, 519-533.
- Schilling, C.H., Letscher, D., and Palsson, B.O. (2000). Theory for the systemic definition of metabolic pathways and their use in interpreting metabolic function from a pathway-oriented perspective. *J Theor Biol* *203*, 229-248.
- Sriram, G., Rahib, L., He, J.S., Campos, A.E., Parr, L.S., Liao, J.C., and Dipple, K.M. (2008). Global metabolic effects of glycerol kinase overexpression in rat hepatoma cells. *Molecular genetics and metabolism* *93*, 145-159.
- Sundaram, T.K., Chell, R.M., and Wilkinson, A.E. (1980). Monomeric malate synthase from a thermophilic *Bacillus*. Molecular and kinetic characteristics. *Archives of biochemistry and biophysics* *199*, 515-525.
- Tserng, K.Y., and Kalhan, S.C. (1983). Calculation of substrate turnover rate in stable isotope tracer studies. *Am J Physiol* *245*, E308-311.
- Zhou, H., Song, X., Briggs, M., Violand, B., Salsgiver, W., Gulve, E.A., and Luo, Y. (2005). Adiponectin represses gluconeogenesis independent of insulin in hepatocytes. *Biochemical and biophysical research communications* *338*, 793-799.